

Evidence for Supersolidity in Bulk Solid ^4He

Xiao Mi,* Anna Eyal, Artem V. Talanov, and John D. Reppy

*Laboratory of Atomic and Solid State Physics and the Cornell Center for Materials Research,
Cornell University, Ithaca, New York 14853-2501*

(Dated: July 6, 2014)

We report low temperature measurements of bulk solid ^4He in a two-frequency compound torsional oscillator with both annular and open cylinder sample geometries. The oscillators were designed to suppress period shifts arising from all known elastic effects of solid ^4He . At temperatures below 0.25 K, period shift signals similar to those reported by Kim and Chan [Science **305**, 1941 (2004)] were observed, albeit two orders smaller in magnitude. A sizable fraction of the observed signals are frequency-independent and consistent with the mass-decoupling expected for supersolid ^4He . This result is in stark contrast with recent works on Vycor-solid- ^4He system and suggests that a small supersolid fraction on the order of 1×10^{-4} may indeed exist in bulk solid ^4He .

PACS numbers: 67.80.Bd, 66.30.Ma

The possible existence of a supersolid, where superflow is supported by the solid phase of ^4He , was suggested more than forty years ago [1–3]. Leggett [3] pointed out that a torsional oscillator (TO) containing a solid ^4He sample would provide an excellent test for the existence of the supersolid state, as the supersolid can be expected to manifest itself in a superfluid-like reduction in the sample moment of inertia, i.e. a non-classical moment of inertia (NCRI). In 2004, Kim and Chan (KC) made TO measurements for Vycor-solid- ^4He [4] and bulk solid ^4He [5] samples and observed anomalous drops in the resonance periods of the TOs below 0.25 K. The KC results were initially interpreted as evidence for NCRI. However, this interpretation was challenged by the discovery, by Day and Beamish (DB) [6], of a temperature-dependent anomaly in the shear modulus, μ , of solid ^4He , occurring over the same temperature range as the KC TO signals as well as sharing the same dependence on velocity/strain and ^3He impurity level. A re-examination by two separate groups [7, 8] of the KC discovery in Vycor-solid- ^4He were recently performed. The conclusion drawn from these experiments is that the original KC period shift observation in Vycor-solid- ^4He arose from the increasing μ of a thin layer of bulk solid ^4He in the TO cells and was unrelated to supersolidity. On the other hand, the possible existence of supersolidity in bulk solid ^4He still remains an open theoretical and experimental question [9].

Multiple-frequency TOs provide an effective method for identifying the origins of the anomalous period shifts below 0.25 K for samples of solid ^4He . In the case of a supersolid NCRI, the fractional period shift (FPS), defined as the anomalous period drop normalized by the mass-loading sensitivity, is expected to be independent of the TO frequency. The FPS is determined by $\Delta P/\Delta P_F$, where ΔP is the magnitude of the anomalous period drop and ΔP_F is the increase in the period of the TO upon freezing of the sample. Should the observed period drop arise from the shear-stiffening of solid ^4He , the FPS would assume different values at different fre-

quencies. The FPS values obtained at different frequencies allow the decomposition of the observed signals into frequency-dependent and frequency-independent contributions. The existence of a finite frequency-independent contribution to the FPS could then indicate the presence of supersolid NCRI.

The shear-stiffening of solid ^4He [6] can alter the TO period in multiple ways, including period shifts arising from the acceleration of solid ^4He [10], stiffening of the solid ^4He in the torsion rods [11], the counter-stress of solid on the cell wall [12] and through the dissipative dynamics of the solid [13]. It is critical in the design of a double-frequency TO that the significant elastic effects should be understood and reduced to a minimum in order to facilitate the analysis of the observed FPS. Such conditions have not been met in the earlier double-frequency experiments on bulk solid ^4He [14, 15]. In these experiments, the FPS signals contained significant contributions from both the acceleration of solid ^4He and the stiffening of solid ^4He inside the torsion rods. In Ref. [16], we reported the preliminary result from a double-frequency TO that was designed to be chiefly sensitive to elastic effect due to acceleration of solid ^4He . In this experiment, a frequency-independent contribution to the FPS was observed that was equivalent to an inertial-mass-decoupling of the cylindrical sample corresponding to a NCRI/supersolid fraction of 1.2×10^{-4} .

The encouraging result from our cylindrical cell [16] prompted a further investigation into the possibility of supersolidity in bulk solid ^4He . In a new experiment, an annular sample geometry was employed which allows a further reduction in the elastic contributions to the FPS signals. Fig. 1 (a) shows the cross-section of the double-frequency TO constructed from annealed Al 6061. The moments of inertia of the cell holding solid ^4He and the dummy oscillator are $I_c = 26.0 \text{ g cm}^2$ and $I_d = 58.7 \text{ g cm}^2$. The corresponding torsion rod constants are $k_c = 1.69 \times 10^9 \text{ dyn cm}$ and $k_d = 1.35 \times 10^9 \text{ dyn cm}$. The torsion rods have inner fill-lines with ra-

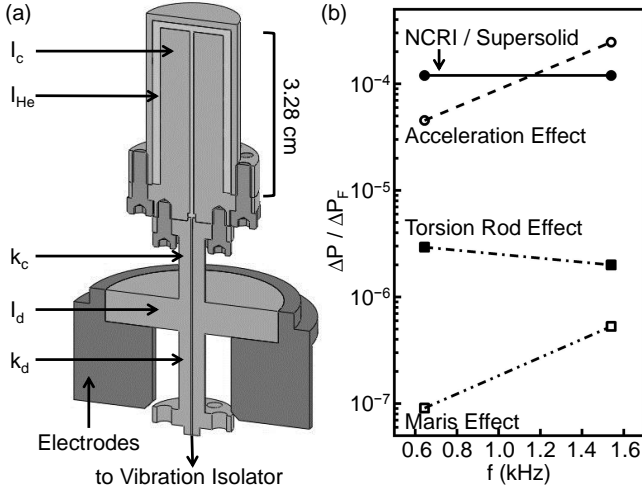


FIG. 1: (a) To-scale drawing of the double-frequency TO. The electrodes for drive/detection of TO motion are constructed from Mg. The rest of the TO is made of annealed Al 6061. (b) Summary of FPS from various effects calculated by varying μ from $1.5 \times 10^8 \text{ dyn cm}^{-2}$ to $3.0 \times 10^8 \text{ dyn cm}^{-2}$, at each frequency of the TO. Value for the acceleration effect is based on FEM computation; the others are analytical estimates.

dius, $r_{\text{fill}} = 0.017 \text{ cm}$ and outer radius $r_{\text{rod}} = 0.256 \text{ cm}$, for a ratio of $r_{\text{fill}}/r_{\text{rod}} = 0.067$. This small ratio greatly reduces the elastic effect from solid ^4He in the fill-lines [11]. The sample is largely annular and has a total solid moment of inertia $I_{\text{He}} = 0.249 \text{ g cm}^2$. A notable improvement in this TO over our previous efforts [7, 16] results from the mounting of the double oscillator on an additional vibration isolator (VI), which is itself a TO with a massive moment of inertia $I_v = 547 \text{ g cm}^2$ and torsion constant $k_v = 1.03 \times 10^9 \text{ dyn cm}$. The VI is in turn mounted to a Cu block that is thermally anchored to the mixing chamber of the dilution refrigerator. The addition of the VI has improved the signal-to-noise ratio by a factor of ten, allowing detection of signals as small as $\Delta P = 0.01 \text{ ns}$, or FPSs on the order of 5×10^{-6} .

In a Supplement to this Letter, we provide detailed calculations of the known elastic effects of solid ^4He for this TO, using both an analytical approach and a finite element method (FEM). Based on these calculations, the estimated FPS values for each elastic effect at the two resonance frequencies are shown in Fig. 1(b). It is clear that, for this annular cell, the only elastic effect on the order of 10^{-4} arises from the acceleration of solid ^4He , with a FPS proportional to f^2 , the square of TO frequency.

We refer the reader to Ref. [7] for a complete description of the drive/detection scheme of the double-frequency TO. The two frequency modes are excited simultaneously with identical maximum rim velocity of $6 \mu\text{ms}^{-1}$ for each mode. We have also driven each mode individually to avoid any nonlinear mode-coupling effects and found the results presented in this Letter to be in-

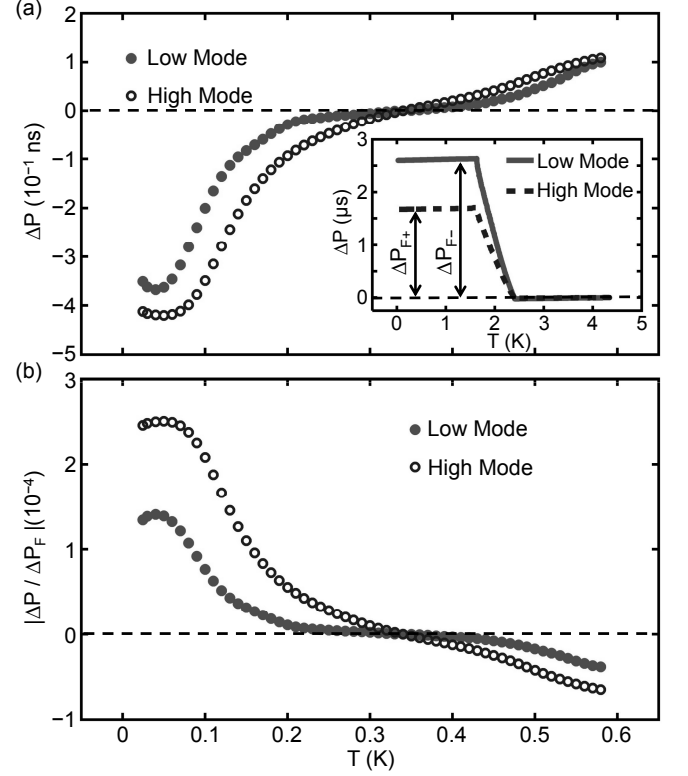


FIG. 2: (a) Period shifts ΔP at each resonance mode, defined as $\Delta P(T) = P(T) - P(T = 0.34 \text{ K})$ where $P(T)$ is the period of the oscillator after correction for the temperature dependent empty cell background. Inset: Period shifts upon freezing of the sample. Mass-loading sensitivities of $\Delta P_{F-} = 2.75 \mu\text{s}$ and $\Delta P_{F+} = 1.69$ are extracted. (b) The magnitude of the FPS is shown as a function of temperature for each mode.

dependent of the method of operation. At $T = 0.5 \text{ K}$, the resonance periods of the empty TO are $P_- = 1.548 \text{ ms}$ for the low frequency ($-$) mode and $P_+ = 0.648 \text{ ms}$ for the high frequency ($+$) mode, with corresponding frequencies of $f_- = 646.0 \text{ Hz}$ and $f_+ = 1543.0 \text{ Hz}$. Since $I_v \gg I_c$ and $I_v \gg I_d$, the influence of the VI on the resonance periods of the TO is small and the two resonance periods are well approximated by $P_{\pm} = 2\pi \left[\frac{I_c(k_c + k_d) + I_d k_c}{2I_c I_d} \left(1 \pm \sqrt{1 - \frac{4I_c I_d k_c k_d}{(I_c(k_c + k_d) + I_d k_c)^2}} \right) \right]^{-1/2}$.

A polycrystalline sample is formed from commercial ^4He gas having a nominal 0.3 ppm ^3He impurity level by the blocked-capillary method. The inset to Fig. 2(a) shows the period shift data for the two resonance modes as the sample is frozen. The total period shifts for the two modes, between the liquid and the solid phase, are $\Delta P_{F-} = 2.75 \mu\text{s}$ and $\Delta P_{F+} = 1.69 \mu\text{s}$. These shifts determine the mass-loading sensitivities for the two modes.

Based on a temperature of 1.63 K at which freezing ceases, the final sample pressure is about 28 bar.

In Fig. 2(a), we present data for the period shift $\Delta P(T)$ at each mode as a function of temperature from $T = 0.02$ K to $T = 0.58$ K. $\Delta P(T)$ is defined taking the cell period at $T = 0.34$ K as the reference value, i.e., $\Delta P(T) = P(T) - P(T = 0.34 \text{ K})$. We observe clear anomalous period drops below 0.2 K where the ΔP decreases rapidly. In the intermediate regime, $0.2 \text{ K} < T < 0.4 \text{ K}$, ΔP shows little variation over temperature. At $T > 0.4$ K, a moderate increase in ΔP is observed which continues to higher temperatures. As a next step, we normalize ΔP at each mode by its mass-loading sensitivity ΔP_F to obtain the FPS. The results are plotted in Fig. 2(b). If the observed signals were attributed entirely to supersolidity, we would expect the FPS to be frequency-independent and depend only on temperature. The two curves in Fig. 2(b) would coincide in this case. This is not the case, with the difference attributable to the elastic effect arising chiefly from the acceleration of the ^4He solid. If the signals arise entirely from the elastic effects of solid ^4He , we would expect the FPS at the two modes to follow the relation $\Delta P_+/\Delta P_{F+} = (f_+/f_-)^2(\Delta P_-/\Delta P_{F-}) \approx 5.7(\Delta P_-/\Delta P_{F-})$, which is also not the case. Therefore, we shall analyze the FPS signals as composites consisting of two components, a frequency-independent component (supersolid fraction) and a component proportional to the square of the frequency arising from dynamic elastic effects.

In decomposing the FPS into individual contributions at each temperature T , we proceed as follows: For each mode, the FPS can be written as $\Delta P_{\pm}(T)/\Delta P_{F\pm} = \Delta P_0(T)/\Delta P_{F\pm} + \Delta P_{1\pm}(T)/\Delta P_{F\pm}$, where $\Delta P_0(T)$ is a temperature-dependent constant and $\Delta P_{1\pm}(T)/\Delta P_{F\pm}$ is the temperature-dependent supersolid contribution to the FPS. The elastic contribution to the FPS is $\Delta P_{1\pm}(T)/\Delta P_{F\pm} = C_0(T)f_{\pm}^2$, where $C_0(T)$ is a temperature-dependent constant. In Fig. 3(a), we plot the elastic contributions to the FPS as a function of temperature. It can be seen that the elastic contribution continues to change above $T = 0.2$ K. This feature is consistent with the continuing change in μ above 0.2 K, and is seen in previous TO experiments that are dominated by elastic effects [7, 18]. Based on a FEM computation described in the Supplement, we deduce that a 50% increase in μ with a base value of $1.5 \times 10^8 \text{ dyn cm}^{-2}$ would produce the observed elastic contributions to the FPS. This is in good agreement with previous measurements of shear-stiffening of solid ^4He , which have reported changes up to 80% [19].

More interesting is the frequency-independent term or supersolid contribution to the FPS shown in Fig. 3(b). Below 0.2 K, this contribution increases to a maximum of 1.2×10^{-4} . As the temperature is raised, the frequency-independent contribution declines and becomes essentially constant between 0.2 K and 0.4 K, suggesting 0.2

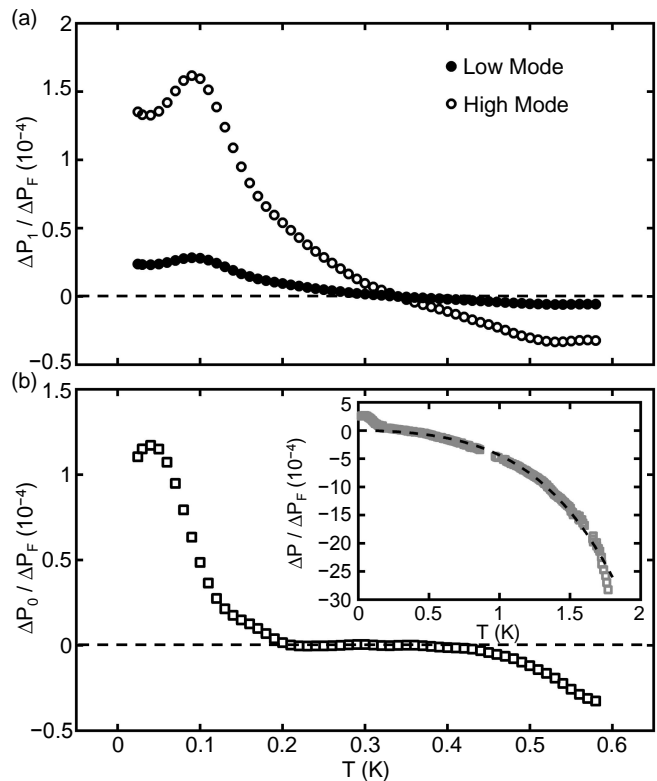


FIG. 3: (a) Elastic, frequency-dependent, contributions to the FPS, $\Delta P_1/\Delta P_F$, at both modes. (b) Supersolid, frequency-independent, contribution to the FPS, $\Delta P_0/\Delta P_F$, identical for both modes. Inset: Total FPS up to melting temperature $\Delta P/\Delta P_F$ for a different sample in a single-mode TO similar in design to the cell used in this experiment. The dashed line, through the data in the inset, is a fit to the functional form of the temperature-dependent variation in solid ^4He pressure [17], $AT^4 + BT^2$.

K as the approximate supersolid transition temperature for this sample. This behavior is consistent with a zero supersolid contribution for $T > 0.2$ K and contrasts with the elastic contribution, which changes continuously over this temperature range. Above 0.2 K, the frequency-independent contribution begins to decline below zero and becomes increasingly negative with increasing temperature. We believe that this trend is explained, in part, by a pressure-induced expansion of the cell. The pressure of constant-volume solid ^4He sample [17] increases as $p(T) = AT^4 + BT^2 + p_0$. As $p(T)$ increases with increasing temperature, the cylindrical walls of the cell are expanded, causing the moment of inertia of the cell, I_c , to increase. The pressure effect becomes much more visible at higher temperatures, as illustrated in the inset of Fig. 3(b), where data from an earlier single-mode TO are shown for temperatures up to 1.8 K.

An instructive way to visualize the data is to plot the period shifts ΔP_{\pm} at different temperatures against each other, as shown in Fig. 4. In the scenario of mass-

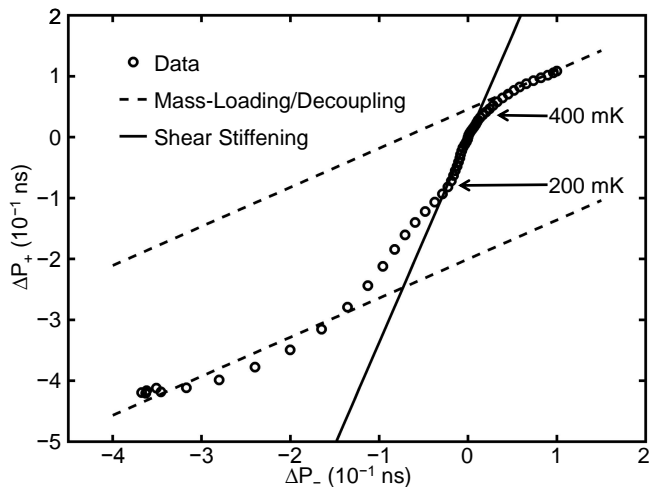


FIG. 4: ΔP_+ against ΔP_- using temperature-dependent values from Fig. 2(a). Slopes corresponding to a mass-loading/decoupling scenario and a solid ^4He shear-stiffening scenario are included.

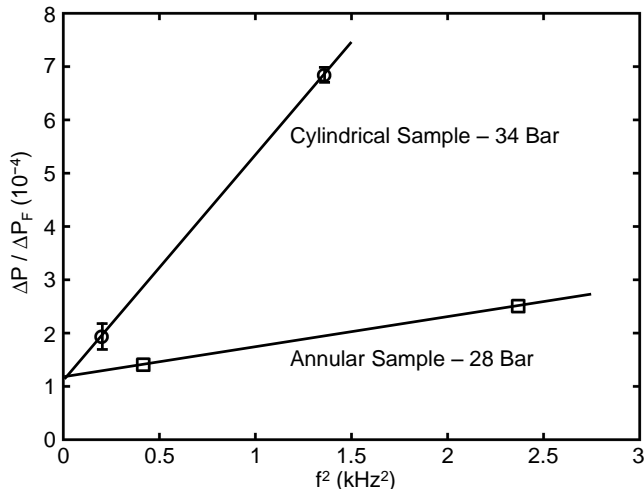


FIG. 5: FPS at $T = 0.02$ K for two double-frequency TO's plotted against f^2 . Error bars are larger in the cylindrical cell due to greater noise level, and are smaller than the size of the symbols for the annular cell.

loading/decoupling, the data would follow a slope equal to the ratio of mass-loading sensitivities, $\Delta P_{F+}/\Delta P_{F-}$. Should the signals arise from shear-stiffening of solid ^4He , the slope would be equal to $(f_+/f_-)^2 \Delta P_{F+}/\Delta P_{F-}$. We see that above 0.4 K, the data follow the mass-loading slope, consistent with pressure-driven expansion of the cell. Between 0.2 K and 0.4 K, the slope of the data is consistent with the expectations based on shear-stiffening of solid ^4He . Below $T = 0.2$ K, the slope of the data returns to a value close to that of mass-decoupling, indicating that the majority of the observed signals, in this temperature range, is due to the presence of supersolidity.

In Fig. 5, we provide a comparison of the results from this annular cell with those from our previous cylindrical cell [16]. For each cell, the FPS at 0.02 K for the low and high modes are plotted against the squares of their respective frequencies, f^2 . We see that the frequency dependence of the FPS is much weaker in the annular cell, as expected due to the greater suppression of the elastic effect arising from inertial acceleration of solid ^4He . The zero-frequency y -intercept gives a non-zero supersolid fraction for both TOs. Despite the complete independence of the two experiments and their difference in geometry, the supersolid fraction is identically $(1.2 \pm 0.1) \times 10^{-4}$.

Since the KC discovery in 2004, TO experiments performed on bulk solid ^4He have reported FPS values ranging from 4×10^{-4} to 0.2 [5, 14, 15, 18, 20–32], with the exceptions of an early spherical TO experiment by Bishop et al [33], which saw no supersolid fraction above 1×10^{-4} , and the rigid TO experiments performed at Penn State [34, 35], which have placed an upper bound of 4×10^{-6} on the supersolid fraction. It is pointed out in [34] that the mass flow observed by Ray and Hallock [36] at low solid pressures, if limited to a flow velocity of $10 \mu\text{m}/\text{sec}$, could lead to FPS on the order 1×10^{-4} , similar to what is observed in their long path-length experiments and in the results we report here. In retrospect, many of the past experiments are heavily influenced by different elastic effects of solid ^4He , leading to recent reports of the non-existence of supersolidity in ^4He [37]. However, the shear modulus anomaly of solid ^4He may very well co-exist, or possibly be correlated, with supersolidity [9]. The small supersolid fraction is simply obscured by huge elastic effects for these experiments. Indeed, the value of the possible supersolid fraction reported here ranks among the smallest seen prior to this work. Therefore, our observation is consistent with the tortuous history of solid ^4He and indicates that a small superflow can persist underneath the giant elastic anomaly. We conclude by noting that the magnitude of the supersolid fraction is consistent with past theoretical predictions [3].

We acknowledge useful and encouraging discussions with P. W. Anderson, W. F. Brinkman and D. A. Huse. This work was supported by the National Science Foundation through Grant DMR-060586 and CCMR Grant DMR-0520404, and partially funded by the New England Foundation, Technion.

* Present Address: Department of Physics, Princeton University, Princeton, NJ 08544, USA

- [1] L. Reatto and G. V. Chester, Phys. Rev. **155**, 88 (1967).
- [2] A. F. Andreev and I. M. Lifshitz, Sov. Phys. JETP **29**, 1107 (1969).
- [3] A. J. Leggett, Phys. Rev. Lett. **25**, 1543 (1970).
- [4] E. Kim and M. H. W. Chan, Nature **427**, 225 (2004).

- [5] E. Kim and M. H. W. Chan, *Science* **305**, 1941 (2004).
- [6] J. Day and J. Beamish, *Nature* **450**, 853 (2007).
- [7] X. Mi and J. D. Reppy, *Phys. Rev. Lett.* **108**, 225305 (2012).
- [8] D. Y. Kim and M. H. W. Chan, *Phys. Rev. Lett.* **109**, 155301 (2012).
- [9] P. W. Anderson, arxiv: 1308.0556 (2013).
- [10] J. D. Reppy, X. Mi, A. Justin, and E. J. Mueller, *J. Low Temp. Phys.* **168**, 175 (2012).
- [11] J. R. Beamish, A. D. Fefferman, A. Haziot, X. Rojas, and S. Balibar, *Phys. Rev. B* **85**, 180501 (2012).
- [12] H. J. Maris, *Phys. Rev. B* **86**, 020502 (2012).
- [13] M. J. Graf, J.-J. Su, H. P. Dahal, I. Grigorenko, and Z. Nussinov, *J. Low Temp. Phys.* **162**, 500 (2011).
- [14] Y. Aoki, J. C. Graves, and H. Kojima, *Phys. Rev. Lett.* **99**, 015301 (2007).
- [15] G. Nichols, M. Poole, J. Nyeki, J. Saunders, and B. Cowan, arXiv: 1311.3110 (2013).
- [16] X. Mi and J. D. Reppy, *J. Low Temp. Phys.* **175**, 104 (2014).
- [17] V. N. Grigor'ev, V. A. Maidanov, V. Y. Rubanskii, S. P. Rubets, E. Y. Rudavskii, A. S. Rybalko, Y. V. Syrnikov, and V. A. Tikhii, *Phys. Rev. B* **76**, 224524 (2007).
- [18] X. Mi, E. J. Mueller, and J. D. Reppy, *J. Phys. Conf. Ser.* **400**, 012047 (2012).
- [19] M. A. Paalanen, D. J. Bishop, and H. W. Dail, *Phys. Rev. Lett.* **46**, 664 (1981).
- [20] A. S. C. Rittner and J. D. Reppy, *Phys. Rev. Lett.* **98**, 175302 (2007).
- [21] A. C. Clark, J. T. West, and M. H. W. Chan, *Phys. Rev. Lett.* **99**, 135302 (2007).
- [22] M. Kondo, S. Takada, Y. Shibayama, and K. Shirahama, *J. Low Temp. Phys.* **148**, 695 (2007).
- [23] A. Penzev, Y. Yasuta, and M. Kubota, *J. Low Temp. Phys.* **148**, 677 (2007).
- [24] A. S. C. Rittner and J. D. Reppy, *Phys. Rev. Lett.* **101**, 155301 (2008).
- [25] A. Penzev, Y. Yasuta, and M. Kubota, *Phys. Rev. Lett.* **101**, 065301 (2008).
- [26] B. Hunt, E. Pratt, V. Gadagkar, M. Yamashita, A. V. Balatsky, and J. C. Davis, *Science* **324**, 632 (2009).
- [27] P. Gumann, D. Ruffner, M. Keiderling, and H. Kojima, *J. Low Temp. Phys.* **158**, 567 (2010).
- [28] J. D. Reppy, *Phys. Rev. Lett.* **104**, 255301 (2010).
- [29] E. J. Pratt, B. Hunt, V. Gadagkar, M. Yamashita, M. J. Graf, A. V. Balatsky, and J. C. Davis, *Science* **332**, 821 (2011).
- [30] D. Y. Kim, H. Choi, W. Choi, S. Kwon, E. Kim, and H. C. Kim, *Phys. Rev. B* **83**, 052503 (2011).
- [31] D. E. Zmeev and A. I. Golov, *Phys. Rev. Lett.* **107**, 065302 (2011).
- [32] A. D. Fefferman, X. Rojas, A. Haziot, S. Balibar, J. T. West, and M. H. W. Chan, *Phys. Rev. B* **85**, 094103 (2012).
- [33] D. J. Bishop, M. A. Paalanen, and J. D. Reppy, *Phys. Rev. B* **24**, 2844 (1981).
- [34] D. Y. Kim, J. T. West, T. A. Engstrom, N. Mulders, and M. H. W. Chan, *Phys. Rev. B* **85**, 024533 (2012).
- [35] D. Y. Kim and M. H. W. Chan, in progress (2014).
- [36] M. W. Ray and R. B. Hallock, *Phys. Rev. Lett.* **100**, 235301 (2008).
- [37] D. Voss, *Physics* **5**, 111 (2012).

Supplementary Material for “Evidence for Supersolidity in Bulk Solid ^4He ”

Xiao Mi,* Anna Eyal, Artem V. Talanov, and John D. Reppy

*Laboratory of Atomic and Solid State Physics and the Cornell Center for Materials Research,
Cornell University, Ithaca, New York 14853-2501*

(Dated: July 7, 2014)

In this Supplement, we provide a more detailed discussion of the effects of shear modulus changes in solid ^4He on the resonance periods of the torsional oscillator (TO) employed in the Letter. We approach the problem with an analytical calculation and a numerical simulation using Finite Element Method (FEM). It is assumed that the absolute value of the shear modulus of solid ^4He is independent of frequency in the frequency range of our TO. This is justified by the measurements of Day et al. [1] who observed a mere 1% variation in the shear modulus of solid ^4He at frequencies between 200 Hz and 2000 Hz.

ANALYTICAL CALCULATION

Acceleration Effect

We first calculate the effect arising from the acceleration field of solid ^4He . The majority of the solid ^4He sample is confined in a long annular channel with inner radius $r_i = 0.635$ cm, outer radius $r_o = 0.794$ cm and height $L = 3.28$ cm. The remaining solid ^4He sample is confined at the top of the sample volume and in a thin cylindrical space with radius $r_c = r_i = 0.635$ cm and height $H = 0.127$ cm.

For the annular part of the sample, the amplitude of the displacement field, \vec{u} , as a function of radius from the symmetry axis of the sample r is calculated to be [2]

$$\vec{u}(r) = \frac{r_m \theta_0 \cos\left((r - r_m)\omega\sqrt{\rho/\mu}\right)}{\cos\left(\frac{1}{2}\Delta r\omega\sqrt{\rho/\mu}\right)} \vec{e}_\theta \quad (1)$$

where $\Delta r = r_o - r_i = 0.159$ cm is the width of the annulus, $r_m = \frac{1}{2}(r_o + r_i) = 0.715$ cm is the mean radius of the annulus, $\omega = 2\pi f$ where f is TO frequency which takes on values of f_- and f_+ at the two resonance modes, ρ and μ are the density and shear modulus of solid ^4He , θ_0 is the maximum angular displacement in radians of the oscillating TO and \vec{e}_θ is the azimuthal direction defined with z -axis being the symmetry axis of the sample. In this estimate, we are neglecting the finite length of the annulus since it is much greater than the radius of the annulus, $L \gg r_m$. The first internal radial sound mode of solid ^4He in this geometry occurs at a frequency of $f_s = \frac{1}{2\Delta r}\sqrt{\mu/\rho} = 86.3$ kHz, nearly two orders of magnitude higher than the TO frequencies. We are therefore

justified in expanding $\vec{u}(r)$ in terms of ω and keeping only the two lowest order terms.

To convert the displacement field into a back-action torque τ_{He} on the TO, we integrate the θ component of the displacement field according to $\tau_{\text{He}} = \int_{r_i}^{r_o} dr \rho \omega^2 u_\theta(r)$ [2, 3]. The effective moment of inertia of solid ^4He is then

$$I_{\text{eff}} = \tau_{\text{He}}/(\theta_0 \omega^2) \approx I_{\text{He}} \left(1 + \frac{1}{2}(\Delta r)^2 \omega^2 \frac{\rho}{\mu}\right) \quad (2)$$

where $I_{\text{He}} = \frac{1}{2}\rho L \pi (r_o^4 - r_i^4) = 0.242$ g cm² is the moment of inertia of the annular part of the ^4He sample. An increase in ^4He shear modulus decreases I_{eff} by an amount $\Delta I_{\text{eff}} \propto \omega^2$, which leads to a fractional period shift (FPS), $\Delta P/\Delta P_F = \Delta I_{\text{eff}}/I_{\text{eff}}$. Therefore, the observed FPS is proportional to f^2 . The cylindrical part of the sample is treated in analogous manner. The effective moment of inertia has a similar form [2]:

$$I_{\text{eff}} \approx I_{\text{He}} \left(1 + \frac{1}{2}H^2 \omega^2 \frac{\rho}{\mu}\right) \quad (3)$$

The moment of inertia of this part of the sample is $I_{\text{He}} = \frac{1}{2}\rho H \pi r_c^4 = 0.0065$ g cm².

To estimate the magnitude of FPS at each resonance mode due to shear-stiffening of solid ^4He , we vary μ from 1.5×10^8 dyn cm⁻² to 3×10^8 dyn cm⁻² and compute the fractional change in the total effective moment of inertia which is the sum of expressions in eqns (2) and (3). The result is a FPS of 1.32×10^{-4} for the high frequency mode and 0.23×10^{-4} for the low frequency mode, both being very close to the elastic contributions to our observed FPS. We note that the 100% increase in ^4He shear modulus may seem unlikely. This is because we have ignored the finite shear modulus of the aluminum alloy constituting the TO. The next effect we discuss takes the elasticity of the cylindrical wall of the cell into account. In the FEM computation presented in the next section, the finite shear modulus of the entire TO is taken into account which amplifies the FPS calculated here, although the FPS remains proportional to f^2 .

Twisting of Cell Walls

In Ref. [2], we discussed a correction to the TO periods due to the twisting of the cell walls. This effect arises from the fact that the top of the cell undergoes a slightly larger angular displacement than the bottom of the cell,

due to the elastic displacement of the cylindrical cell wall. The size of this effect is approximated by changes in the effective moment of inertia I_E of the cell itself, which is given by

$$I_E \approx I_U \left(1 + \frac{1}{3} U^2 \omega^2 \frac{\bar{\rho}}{\bar{\mu}} \right) \quad (4)$$

where $I_U = 7.05 \text{ g cm}^2$ is the moment of inertia of the cell from the bottom of the solid ^4He sample to the top, $U = 3.43 \text{ cm}$ is the total length of this part of the cell, $\bar{\rho}$ and $\bar{\mu}$ are the weighted averages of the density and shear modulus of the cell+ ^4He system. Specifically for our cell, since $I_U \gg I_{\text{He}}$, $\bar{\rho} \approx \rho_{\text{al}}$ where $\rho_{\text{al}} = 2.7 \text{ g cm}^{-3}$ is the density of aluminum. $\bar{\mu}$ is given by considering the cross-section of the sample space. At radius $r < 0.635 \text{ cm}$ and $0.794 \text{ cm} < r < 0.921 \text{ cm}$, the cross-section is occupied with aluminum. Solid ^4He only occupies the annular region $0.635 \text{ cm} < r < 0.794 \text{ cm}$. Approximating the cell as a torsion rod with this given cross-section, we calculate that the fractional contribution of solid ^4He to the total torsion constant is $0.48\mu/\mu_{\text{al}}$ where $\mu_{\text{al}} = 2.9 \times 10^{11} \text{ dyn cm}^{-2}$ is the low temperature shear modulus of Al 6061 alloy. This suggests that $\bar{\mu} \approx \mu_{\text{al}} + 0.48\mu$.

As before, we vary μ from $1.5 \times 10^8 \text{ dyn cm}^{-2}$ to $3 \times 10^8 \text{ dyn cm}^{-2}$, obtaining a change in I_E of $\Delta I_{E-} = 1.05 \times 10^{-6} \text{ g cm}^2$ for the low frequency mode and $\Delta I_{E+} = 6.01 \times 10^{-6} \text{ g cm}^2$ for the high frequency mode. Normalizing these values by the moment of inertia of solid ^4He , I_{He} , the FPS is 4.23×10^{-6} for the low frequency mode and 2.41×10^{-5} for the high frequency mode. We note that this effect has the same f^2 dependence as the acceleration effect. Comparing the values of the FPS calculated here to those calculated for the acceleration effect, we see the finite shear modulus of the cylindrical cell wall alone enhances the acceleration effect by about 20%.

Torsion Rod Effect

The effect on TO periods produced by the stiffening of solid ^4He inside the fill-line drilled through the torsion rods is minimized by reducing the radius of the fill-line, r_{fill} . For our torsion rods which have outer radius r_{rod} and shear modulus μ_{al} , the FPS produced by a change in solid ^4He shear modulus $\Delta\mu$ is [4], in the limit of $r_{\text{fill}} \ll r_{\text{rod}}$,

$$\frac{\Delta P_{\pm}}{\Delta P_{\text{F}\pm}} \approx \frac{P_{\pm}}{2\Delta P_{\text{F}\pm}} \frac{\Delta\mu}{\mu_{\text{al}}} \left(\frac{r_{\text{fill}}}{r_{\text{rod}}} \right)^4 \quad (5)$$

For our TO, $r_{\text{fill}}/r_{\text{rod}} = 0.067$. The measured mass-loading sensitivities are $\Delta P_{\text{F}-} = 2.75 \text{ }\mu\text{s}$ and $\Delta P_{\text{F}+} = 1.69 \text{ }\mu\text{s}$. Assuming the shear modulus of solid ^4He changes by 100% so that $\Delta\mu = 1.5 \times 10^8 \text{ dyn cm}^{-2}$, the FPS is 2.94×10^{-6} for the low frequency mode and 2.00×10^{-6} for the high frequency mode. Since these

estimates are two orders of magnitude smaller than the measured signals, we conclude that the solid ^4He inside the torsion rods forms negligible contribution to the observed FPS.

Maris Effect

A subtle effect was discussed by H. J. Maris [5] where the solid ^4He sample inside the TO cell modifies the torsion constant of the torsion rod by exerting a counter-stress on the deformed cell wall separating solid ^4He from the torsion rod. This ‘‘Maris effect’’ is much more significant for solid ^4He samples with cylindrical geometries than for those with annular geometries. To estimate the size of such an effect in our annular cell, we replace the inner Al cylinder of the cell by solid ^4He , so that the solid ^4He sample is a cylinder with height $L = 3.28 \text{ cm}$ and radius $r_o = 0.794 \text{ cm}$. The result from this simplification is an upper bound on the magnitudes of the signals if the actual geometry is used.

Following the approach outlined in Ref. [5], we calculate that for a change of $\Delta\mu$ in solid ^4He shear modulus, the corresponding change in the torsion constant k_c of the cell Δk_c is

$$\Delta k_c = 3.2 \times 10^{-9} (\Delta\mu/\mu) k_c \quad (6)$$

It is noteworthy that the Maris effect only affects the torsion constant of the cell, whereas the torsion rod effect affects the torsion constants of both the cell and the dummy oscillator. Consequently, the frequency dependences of the two effects are different.

The induced period shifts ΔP_{\pm} are obtained by increasing k_c by an amount Δk_c and calculating the decrease in the TO periods $P_{\pm} = 2\pi \left[\frac{I_c k_c + I_c k_d + I_d k_c}{2I_c I_d} \left(1 \pm \sqrt{1 - \frac{4I_c I_d k_c k_d}{(I_c k_c + I_c k_d + I_d k_c)^2}} \right) \right]^{-1/2}$. For a 100% change in μ , the period shifts are $\Delta P_- = 2.5 \times 10^{-4} \text{ ns}$ and $\Delta P_+ = 9.0 \times 10^{-4} \text{ ns}$. These values give FPS of 9.1×10^{-8} for the low frequency mode and 5.3×10^{-7} for the high frequency mode, both being more than two orders of magnitude smaller than the observed FPS.

Dissipation of Solid ^4He

The additional dissipation introduced by the solid ^4He in our experiment is very small. The increase in $1/Q$ where Q is the mechanical quality factor of the TO after the cell is filled with solid ^4He has a peak value of only 5×10^{-8} around a temperature of 0.1 K for both modes. The shifts in resonance periods associated with such changes in dissipation are $\Delta P_- = 3.87 \times 10^{-9} \text{ ns}$ and $\Delta P_+ = 1.62 \times 10^{-9} \text{ ns}$. These values correspond to FPS of 1.41×10^{-12} for the low frequency mode and 0.96×10^{-12} , eight

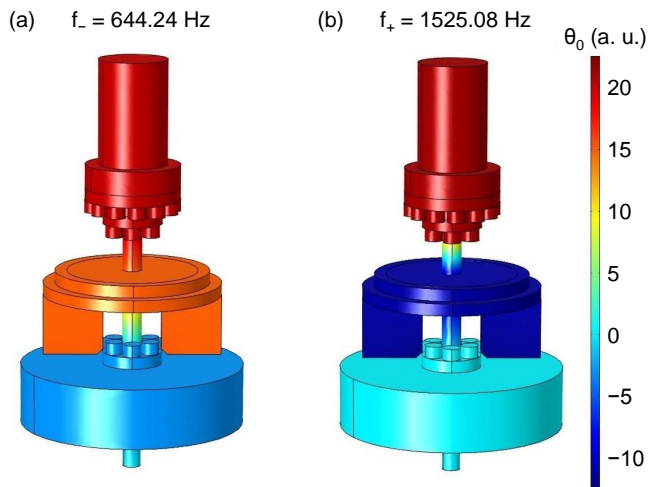


FIG. 1: (Color Online) FEM simulations of the amplitude of angular displacements θ_0 and resonance frequencies f_{\pm} of the two resonance modes of the annular TO used in the Letter. All dimensions used in building the FEM model are the measured values of the actual apparatus. θ_0 is plotted in arbitrary units. The bottom oscillator is the vibration isolator.

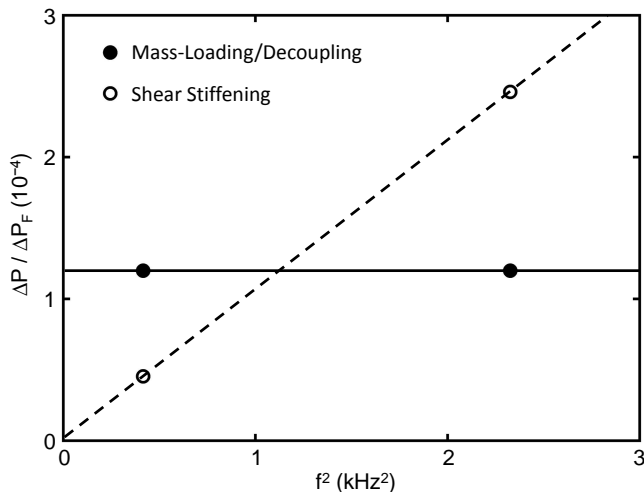


FIG. 2: FEM computations of FPS's ($\Delta P / \Delta P_F$) for the annular TO, based on a fractional change of 1.2×10^{-4} in the density of solid ^4He sample alone, and based on a 100% increase in the shear modulus of solid ^4He sample alone.

orders of magnitude smaller than the FPS measured in the experiments.

FEM COMPUTATIONS

FEM calculations of TO resonance periods are performed with commercial software package COMSOL Multiphysics (structural mechanics module, COMSOL Multiphysics v4.3b, COMSOL Inc., 2013). A mesh consisting of 20745 domain elements is created, and the pro-

gram solves for the eigen-frequencies ω of the Navier-Cauchy equation for the amplitude of the displacement field, \vec{u} , of the entire TO:

$$-\rho\omega^2\vec{u} - \nabla \cdot \bar{\sigma} = 0 \quad (7)$$

where $\bar{\sigma}$ is the stress tensor. A plot for the amplitude of angular displacement, θ_0 , at the two resonance modes is shown in Figure. 1. We have included the vibration isolator in the model for added precision. It can be seen that the values of θ_0 have the same sign at the cell and the dummy oscillator for the low frequency mode, but opposite signs at the high frequency mode. Hence the two modes have shapes expected from analytical calculations, where the cell and the dummy oscillator rotate in-phase at the low frequency mode and out-of-phase at the high frequency mode. From the values of θ_0 , we also extract the scale factors D_{\pm} relating the angular velocity of the dummy oscillator $\dot{\theta}_d$ to that of the cell $\dot{\theta}_c$, $\dot{\theta}_c = D_{\pm}\dot{\theta}_d$, which turns out to be $D_- = 1.40$ and $D_+ = -1.65$. From Figure. 1, one can see the eigen-frequencies calculated by the program match those measured experimentally very closely. We also check for the accuracy of the model by varying the density of solid helium ρ from 0 to 0.2 g cm^{-3} . The calculated shifts in resonance periods are $2.76 \mu\text{s}$ and $1.72 \mu\text{s}$ for the low and high frequency modes respectively, again matching the experimental values ΔP_{F-} and ΔP_{F+} .

To study the effect of changing solid ^4He shear modulus μ , we shift the value of μ from $1.5 \times 10^8 \text{ dyn cm}^{-2}$ to $3 \times 10^8 \text{ dyn cm}^{-2}$ and calculate the shifts in periods at the two modes, ΔP_{\pm} . Normalizing these shifts by the mass-loading values $\Delta P_{F\pm}$, the calculated FPS are 0.454×10^{-4} for the low frequency mode and 2.46×10^{-4} for the high frequency mode. These values are about twice those calculated with the analytical approach and likely to be quantitatively accurate, since the finite shear modulus of the entire TO is taken into account. They also suggest that a 50% change in the shear modulus is sufficient to account for the elastic contribution to the FPS observed in this experiment.

An important message imparted by the FEM simulation is the frequency dependence of the signals produced by the changing shear modulus of solid ^4He . The ratio of the computed FPS at the two modes is $2.46/0.454 = (f_+/f_-)^{1.96}$. The exponent of 1.96 is in excellent agreement with the analytical prediction of 2, suggesting that changing solid ^4He shear modulus indeed produces a FPS that is proportional to f^2 for the cell presented in the Letter. To visualize such a frequency dependence, we plot the computed FPS values based on changes in μ in Figure. 2 as a function of f^2 . The values are seen to extrapolate to $< 10^{-5}$ in the zero-frequency limit. In contrast, the value of FPS based on a supersolid fraction of 1.2×10^{-4} is seen to be independent of frequency. Comparing the FEM computation to data presented in

Figure. 5 of the Letter, we see that the experimental FPS values can only arise from a combination of both effects.

* Present Address: Department of Physics, Princeton University, Princeton, NJ 08544, USA

- [1] J. Day and J. Beamish, *Nature* **450**, 853 (2007).
- [2] J. D. Reppy, X. Mi, A. Justin, and E. J. Mueller, *J. Low Temp. Phys.* **168**, 175 (2012).
- [3] M. J. Graf, J.-J. Su, H. P. Dahal, I. Grigorenko, and Z. Nussinov, *J. Low Temp. Phys.* **162**, 500 (2011).
- [4] J. R. Beamish, A. D. Fefferman, A. Haziot, X. Rojas, and S. Balibar, *Phys. Rev. B* **85**, 180501 (2012).
- [5] H. J. Maris, *Phys. Rev. B* **86**, 020502 (2012).